Journal Pre-proofs

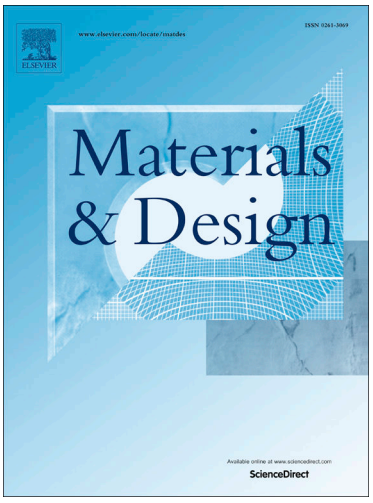

Hygrothermal aging behavior of biochar-reinforced polylactide/wood plastic composites

Yu Xian, Shenhao Li, Xia Yang, Haixin Peng, Ruyan Zhang, Hongbo Li, Zebing Xing, Ge Wang, Haitao Cheng

PII: S0264-1275(25)01456-X
DOI: https://doi.org/10.1016/j.matdes.2025.115035
Reference: JMADE 115035

To appear in: *Materials & Design*

Received Date: 1 September 2025
Revised Date: 22 October 2025
Accepted Date: 27 October 2025

Please cite this article as: Xian, Y., Li, S., Yang, X., Peng, H., Zhang, R., Li, H., Xing, Z., Wang, G., Cheng, H., Hygrothermal aging behavior of biochar-reinforced polylactide/wood plastic composites, *Materials & Design* (2025), doi: https://doi.org/10.1016/j.matdes.2025.115035

Hygrothermal Aging Behavior of Biochar-Reinforced Polylactide/Wood Plastic Composites

Yu Xian [a*], Shenhao Li [a],Xia Yang [a],Haixin Peng [b], Ruyan Zhang [a], Hongbo Li [c], Zebing Xing [c], Ge Wang[d], Haitao Cheng [d*]

[a] College of Forestry, Shanxi Agricultural University, Taigu, Shanxi, 030801, China

[b] Department of Biosystems Engineering, College of Engineering Auburn University, Auburn, 36849,USA

[c] College of Agricultural Engineering, Shanxi Agricultural University, Taigu, Shanxi, 030801, China

[d] Key Laboratory of National Forestry and Grassland Administration on Bamboo & Rattan Science and Technology, International Centre for Bamboo and Rattan, Beijing 100102, China

*Correspondence: Yu Xian, xianyu_sxau@126.com; Haitao Cheng, cheng_icbr@126.com

Abstract: Addressing the need for sustainable materials amid growing environmental concerns, this study investigates the development of biodegradable composites from landscaping waste (LW) and polylactic acid (PLA), enhanced with biochar (BC). The primary focus is on evaluating the impact of BC addition (0.5-4wt%) on the mechanical performance and hygrothermal aging (water absorption and color stability) of LW/PLA composites. Furthermore, BC incorporation effectively mitigates aging: increasing BC content and exposure time lead to lower thickness swelling, reduced color fading, and less surface deterioration compared to BC-free composites. Water absorption kinetics followed the Fickian model, and saturation significantly degraded mechanical properties, primarily due to fiber swelling, interfacial micro-cracking, and debonding. Dynamic mechanical analysis confirmed that moisture saturation increased the loss factor and impaired interfacial stress transfer. This work demonstrates that BC, particularly at 1%, is a highly effective modifier for enhancing the performance and durability of sustainable LW/PLA composites.

Keywords: Biochar; Landscaping waste; Biodegradable composites; Water absorption aging; Mechanical performance; Dynamic mechanical analysis

1 Introduction

The rapid development of industrialization has driven an escalating demand for non-renewable energy sources, such as oil and coal, contributing to severe global environmental challenges. Concurrently, global forest resources are diminishing, while China's demand for wood resources continues to rise annually. In 2020 alone, over 390 million tons of plastics were produced for applications spanning industrial and residential construction, transportation, and other sectors. However, improper disposal and the non-biodegradable nature of these plastics have significantly exacerbated global pollution (Shih et al., 2024; Zhao,You, 2024). To mitigate these pressing issues, the development of sustainable materials is urgently needed.

Wood-plastic composites (WPCs) present a promising alternative. They are manufactured by combining plant fibers (e.g., wood flour, rice husk, bamboo powder) with synthetic resins (e.g.,

polyethylene, polypropylene, polyvinyl chloride) through processes like hot pressing, extrusion, or injection molding (Espinachet al., 2024; Lv et al., 2018; Shirinbayan et al., 2024). WPCs integrate the advantages of both wood fibers and plastics, offering benefits such as good dimensional stability, resistance to cracking, and tolerance to acids and alkalis (Bazliet al., 2022;Siakeng et al., 2019). Consequently, they are gaining significant traction in diverse industries including aerospace, home decoration, and logistics, demonstrating considerable application potential (Kamarudin et al., 2022).

A critical factor influencing WPC durability is the inherent incompatibility between the hydrophilic surfaces of natural fibers, rich in polar groups, and the typically non-polar thermoplastic matrices (Jubinville et al., 2024; Mohammed et al., 2022; Xie et al., 2010; Zhou et al., 2016). To address this, researchers often incorporate high-performance fillers like carbon nanotubes, graphene, or carbon fiber (Y. Zhang et al., 2020). Bamboo charcoal (BC), sharing unique functionalities with carbon materials like carbon fiber and carbon black, has recently emerged as a widely used filler in composites. Studies on BC-reinforced composites have demonstrated its effectiveness in improving interfacial adhesion and enhancing the structural-mechanical properties of WPCs and polylactic acid (PLA) composites (Das et al., 2015, 2016; X. Li et al., 2014; Ho,Lau, 2014; Ho et al., 2015;). Furthermore, research has investigated the properties of biodegradable polymer composites by analyzing factors such as BC loading and particle size, revealing reinforcement mechanisms primarily involving the polymer matrix embedding into BC pores to form an interlocking structure that enhances interfacial interaction and composite performance (Naeem et al., 2017; S. Li et al., 2018; Q. Zhang et al., 2020). BC has also been shown to improve the electrical conductivity and electromagnetic shielding properties of biomass/HDPE composites (Yang et al., 2018).

However, the long-term performance of WPCs in practical applications is significantly challenged by hygrothermal aging, which adversely affects mechanical properties, dimensional stability, and service life. Water absorption in WPCs is influenced by fiber content, plastic matrix type and content, fiber size/shape, interfacial compatibility, and the presence of fillers (Duigou et al., 2009;Hao et al., 2020; Stark et al., 2004;). Comparative durability assessments under identical environmental conditions revealed that wood fiber reinforced PLA composites (both semi-crystalline and amorphous) exhibit higher moisture absorption and more significant dimensional changes and mechanical property degradation than short carbon fiber reinforced ABS (CF/ABS) (Saavedra-Rojas et al., 2024). While treatments like drying or coupling agents can improve the anti-aging properties of plant fiber composites (Q. Li et al., 2022), temperature and wood flour content remain critical factors influencing WPC water absorption (W. Wang et al., 2020). Recent findings suggest that optimal BC addition can enhance thermal stability, flame retardancy, and reduce water absorption and thickness swelling in composites (Hoang et al., 2024; Zhu et al., 2020), as evidenced by improvements in epoxy resin and sisal-reinforced vinyl ester composites (Dahal et al., 2023; Sivamurugan et al., 2024).

Despite these advances, conventional WPCs predominantly rely on non-biodegradable polymers (e.g., PE, PP) and virgin wood fibers, raising concerns regarding environmental persistence and resource sustainability. Although biodegradable alternatives, such as PLA-based WPCs, have been explored, critical research gaps persist: i) abundant and low-cost resources like

landscaping waste (LW) are rarely employed in WPCs; ii) PLA/LW composites suffer severe hydrolytic degradation and mechanical decay under wet conditions due to poor interfacial adhesion; iii) existing strategies to enhance durability (e.g., chemical treatments) often compromise biodegradability. To address these gaps, this study proposes BC as a multifunctional eco-modifier derived from carbon-negative processes. We hypothesize that BC can: (i) upgrade LW into a value-added reinforcement, (ii) strengthen PLA/LW interfaces, and (iii) mitigate water-driven aging while preserving full biodegradability.

This study aims to systematically elucidate the synergistic optimization mechanism of gradient-regulated BC addition (0.5%-4%) on the hygrothermal aging resistance of PLA-based WPCs incorporating LW. Through multi-dimensional characterization-assessing mechanical properties (flexural strength, impact strength), hygroscopic behavior (water absorption, thickness swelling rate), apparent color stability, and dynamic thermomechanical properties, we will quantitatively analyze the intrinsic relationship between moisture absorption kinetics and interfacial structure evolution using Fickian diffusion models. This research will elucidate the dual-pathway mechanism by which BC enhances aging resistance through interface reinforcement and moisture diffusion inhibition. Ultimately, the quantitative relationship between BC loading levels and composite performance responses will be established, providing theoretical and technical foundations for developing eco-friendly WPCs with improved weather resistance and reduced environmental sensitivity.

2 Materials and methods

2.1 Materials

Landscaping Waste (LW): Raw materials consisting of dead and pruned branches (primarily poplar wood) were collected from landscaping activities at Shanxi Agricultural University in 2024. The poplar-based LW primarily contains cellulose (42.35%), hemicellulose (24.45%), lignin (23.27%). The collected branches were processed through crushing, sieving, and grinding to obtain wood powder with a particle size of 100 mesh. The physical appearance of LW before and after grinding is illustrated in Figure1. Polylactic Acid (PLA): PLA resin (grade 4032D) was supplied by Dongguan Huachuang Plastic Products Company. Biochar (BC): Bamboo-derived biochar (particle size: 100 mesh; specific surface area: 7462.52 m^2/g; pore volume: 5.6976 mL/g; average pore size: 3.0540 nm) was procured from Fujian Xinsen Carbon Industry Co., Ltd.

2.2 Preparation of composite materials

LW powder was drying at 80°C for 24 hours to achieve a moisture content below 2%. The dried powder (100 mesh) was then compounded with polylactic acid (PLA) and biochar (BC). BC was incorporated at loading levels of 0.5-4 wt%. The constituent materials (poplar powder, PLA, BC) were precisely weighed using an analytical balance (±0.001 g accuracy) to ensure accurate weight fractions. The dry-mixing process was repeated three times to verify homogeneity.

The mixture was subsequently melt-compounded using a single-screw extruder. To mitigate the inherent brittleness of PLA, the extrusion temperature profile was carefully controlled to avoid thermal degradation and ensure uniform melting. The extruder screw velocity was precisely regulated at 30 rpm to minimize shear-induced chain scission and preserve molecular weight. The extruder barrel comprised three temperature zones set at 50 °C (feed zone), 145 °C, and 155 °C

(die zone). The extruded strands were pelletized using a strand pelletizer, resulting in granules with an average length of 2-3 mm and a diameter of 2 mm.

The compounded pellets were then molded into test specimens using a hot press (plate vulcanization machine) under typical conditions (temperature 170 °C, and pressure 10 MPa for 10 minutes).

A control composite without BC addition (LW/PLA only) was also prepared following the same procedure. The overall composite manufacturing workflow is illustrated in Figure 1. The detailed composition design of BC-reinforced LW/PLA composites are provided in Table 1.

Figure 1 Manufacturing workflow for BC-reinforced LW/PLA composites

Table 1 Composition design of BC-reinforced LW/PLA composite

2.3 Mechanical properties test

While flexural and impact properties are critical for assessing composite performance in structural applications, this study focused on these two tests due to their relevance to real-world loading conditions. Flexural characterization was conducted per ASTM D790-10 using a three-point bending fixture with 60mm support span. Tests employed 5 mm/min crosshead displacement on specimens (80 × 12.7 × 2.2 mm^3). Five replicates yielded mean flexural properties.

Impact strength was determined by the Charpy impact test (simply supported beam method) according to ASTM D6110-10. Specimen dimensions were 127 × 12.7 × 2.2 mm^3. Five replicates yielded are reported as the average value.

2.4 Water absorption test

Water absorption behavior was characterized per ASTM D 570-98 using rectangular specimens 76.2 mm × 25.4 mm × 2.2 mm. Prior to testing, all LW/PLA composite specimens underwent 8-hour conditioning at 110℃ in a forced-convection oven. Initial dry mass (m_0) was recorded via analytical balance (precision: ±0.01g). Specimens with varying BC content were subsequently immersed in distilled water maintained at 25℃. At predetermined immersion times (t), specimens were removed from the water. Surface moisture was carefully blotted off using filter paper. The mass (m_t) was immediately weighed, and the material thickness was measured at pre-marked positions on the specimen surface. The average thickness at each time point (H_t) was calculated. The initial average thickness (H_0) was determined by measuring the pre-marked positions on dry specimens prior to immersion. Thickness swelling (TS, %) and water absorption (WA, %) were quantified via Equations (1) and (2) respectively. Measurements continued periodically from immersion until saturation was reached. For each material group, five replicate specimens were tested, and the average values of TS and WA are reported.

$$TS = (H_t - H_0)/H_0 \times 100\% \quad (1)$$

$$WA = (m_t - m_0)/m_0 \times 100\% \quad (2)$$

2.5 Color difference analysis

Specimens measuring 25 mm × 25 mm were sectioned from the composite material. The color of the aged surface was measured using a colorimeter. Untreated specimens served as the reference standard. Color indices (L^*, a^*, b^*) were then measured on specimens subjected to different aging durations. Triplicate measurements at strategically distributed positions on each specimen yielded mean values. The total color difference (ΔE^*) was derived from Equation (3) following CIE LAB conventions:

$$\Delta E^* = \sqrt{(L_1^* - L_0^*)^2 + (a_1^* - a_0^*)^2 + (b_1^* - b_0^*)^2} = \sqrt{(\Delta L^*)^2 + (\Delta a^*)^2 + (\Delta b^*)^2} \quad (3)$$

Where ΔE^* is the total color difference, L^* represents lightness (0 = black, 100 = white), a^* represents the red-green axis (positive = red, negative = green), b^*represents the yellow-blue axis (positive = yellow, negative = blue). ΔL^*, Δa^*, Δb^* are the differences in the respective color coordinates between the aged specimen and the untreated reference specimen.

2.6 DMA analysis

In this paper, DMA analysis of LW/PLA composites was performed using a NETZSCH DMA 242 instrument (Germany). Tests employed dual cantilever mode at 25°C with rectangular specimens (60 mm×8 mm×2.2 mm). Temperature sweeps from ambient to 120°C were executed at 1 Hz oscillation frequency and 30 μm strain amplitude.

2.7 SEM analysis

Scanning electron microscopy (SEM) characterized topographical evolution and microstructural alterations in composites pre- and post-hydration. Specimen surfaces were gold-sputtered to mitigate charging effects prior to imaging. Observations employed 3.0 kV accelerating voltage. The SEM micrographs were used to qualitatively assess the dispersion uniformity of BC particles within the PLA matrix and to identify the presence of voids, agglomerations, and interfacial defects.

3 Results and discussion

3.1 BC contents on mechanical properties in composites

3.1.1 Static mechanical properties

Figure 2 delineates BC content-dependent variations in mechanical performance of LW/PLA composites under hygrothermal aging. Notably, Figure 2a reveals the elastic modulus increased by 14.90%, 10.52%, 13.47%, 12.95%, and 7.07% compared to the BC-free composite. Although the flexural modulus increased with BC addition compared to the BC-free composite, the modulus at 1% BC was slightly lower than that at 0.5% and 2% BC. This may be attributed to the optimal dispersion and interfacial bonding at 1% BC, which enhances toughness but slightly compromises stiffness compared to higher BC loadings where rigid filler dominance increases modulus. At 1%

BC content, the flexural strength peaked at 25.16 MPa, representing a 19.20% increase over the control group. However, further increases in BC content led to a decline in flexural strength. While BC's inherent rigidity enhances composite stiffness, excessive content promotes particle agglomeration. This agglomeration overrides the reinforcement mechanism where molten PLA infiltrates BC micropores during processing, forming encapsulated structures that enable efficient stress transfer via mechanical interlocking – as reported for PLA and other thermoplastics (Shah et al., 2023; Wei et al., 2022; C. Das et al., 2021). At 1% BC, peak flexural strength arises from synergistic bridging of poplar cellulose microfibrils by well-dispersed BC particles, optimizing stress distribution through the PLA matrix. In contrast, 4% BC composites exhibit agglomerate-induced failure: particle clustering disrupts the cellulose-BC network and creates weak interfaces, particularly in lignin-rich regions where poor BC adhesion initiates premature fracture.

Following equilibrium water absorption at room temperature, both flexural strength and modulus decreased by over 50%. The degree of mechanical property degradation initially increased then decreased with rising BC content, with the most significant reduction observed at 2% BC. Hygroscopic aging likely weakens the fiber-PLA interface bond due to plant fiber expansion/shrinkage, promoting micro-crack and pore formation (Bao, 2018; José et al., 2016; Oliveira et al., 2022). Concurrently, water penetration swells and softens the resin matrix, potentially disrupting molecular chains, chemical crosslinking, and the material's network structure.

Figure 2 Flexural and impact properties of composites in dry versus water-saturated states: (a) flexural properties (b) impact properties.

As depicted in Figure 2b, the impact strength of dry composites initially rose then fell with increasing BC content. A 1% BC addition yielded peak impact strength (2.63 kJ /m², +3.06%). Subsequent reductions suggest that excessive BC increases material rigidity while diminishing toughness, adversely affecting impact performance (Qingfa et al., 2021). After water absorption saturation, impact strength generally decreased, except for the 2% BC formulation.

Notably, the reduction in impact strength post-absorption was less severe than for flexural strength. This divergence arises because water molecules act as a plasticizer within the cellulose network. Penetrating the amorphous regions, they increase polymer chain mobility and reduce deformation resistance. Although this irreversibly disrupts hydrogen bonding-compromising stiffness and flexural strength, it simultaneously enhances toughness and energy absorption (Dhakal et al., 2007; Randhawa et al., 2021). Consequently, the composite retains higher impact resistance despite water saturation. Impact strength involves high-energy, single-event loading, making it less sensitive to plastic deformation effects than sustained flexural loading. Composites with 2% BC exhibited the lowest flexural and impact strengths after absorption. This is likely due to their higher water uptake and poorer interfacial compatibility. Severe hydrolysis damage at the interface early in aging may prevent effective diffusion and transmission of impact stress, explaining the consistently low impact strength and the poorest flexural performance in this group.

3.1.2 Dynamic thermo-mechanical properties

Figure 3 and Table 2 compare the glass transition temperature (T_g) and tan δ peak behavior of composites in dry versus water-saturated states. For LW/PLA composites reinforced with varying BC content, the storage modulus (E') of dry samples was significantly higher than that of hygroscopic samples.

In the dry state, E' increased with BC addition compared to the BC-free composite. At 1% BC content, E' reached a maximum of 3018.84 MPa, representing a 186% increase over the BC-free composite (1055.46 MPa). This enhancement in E' is attributed to synergistic mechanisms induced by BC, including rigid filler reinforcement, interfacial strengthening (facilitated by its high specific surface area and porous structure), regulation of PLA crystalline structures (acting as nucleating agents), and restriction of molecular chain mobility (via physical crosslinking). These mechanisms collectively improve the composite's elastic response and structural rigidity under dynamic loading.

As shown in Figure 3a-f, upon reaching equilibrium water absorption, the glassy-state E' decreased by 61.97%, 48.25%, 72.32%, 73.23%, 72.08%, and 73.41%, respectively. This trend aligns with the degradation observed in static mechanical properties (impact and flexural strength). Water absorption induces molecular chain scission within the composite system, reducing material rigidity and accelerating the degradation of both static and dynamic mechanical properties.

For dry samples, the tan δ peak value decreased with increasing BC content. Compared to the BC-free composite,The tan δ peak in BC-free composites indicates heterogeneous mobility of hemicellulose-bound polymer chains. tan δ decreased by 66.67% at 1% BC content. Beyond this, tan δ values varied minimally among BC contents but remained consistently lower than the control. The overall tan δ trend before and after hygroscopic aging was similar: tan δ increased slowly at lower temperatures, rose rapidly near ~60 °C to a peak, then declined. In some samples, tan δ plateaued in the final stage. The tan δ peak reflects the magnitude of energy dissipation during dynamic deformation, with its corresponding temperature indicating the material's T_g.

After water absorption, the tan δ peak shifted to lower temperatures across all samples. Concurrently, the peak height of wet specimens consistently exceeded that of their dry counterparts. As indicated in Table 2, a clear downward trend in T_g was observed. This reduction in is attributed to disruption of the polymer crosslinking network integrity within the resin matrix (Jagadeesh et al., 2023). and depressed T_g confirm the plasticization effect of water molecules on the polymer network (Célino et al., 2013). The increase in tan δ peak height post-absorption primarily stems from hygrothermal aging: differential thermal and hygroscopic expansion coefficients between fibers and resin generate interfacial shear stress, weakening interfacial bonding strength (Wu et al., 2021). Concurrently, water molecules plasticize the polymer crosslinked network, reducing resistance to molecular chain movement and further elevating the tan δ peak.

Figure 3 Dynamic thermo-mechanical properties of composites in dry versus water-saturated states: (a) LW/PLA-0 (b) LW/PLA-0.5 (c) LW/PLA-1 (d) LW/PLA-2 (e) LW/PLA-3 and (f)LW/PLA-4.

Table 2 T_g and tanδ of samples before and after water absorption

3.2 BC contents on water absorption and diffusion behaviors in composites

3.2.1 BC contents on water absorption in composites

Accelerated water immersion testing quantified long-term dimensional stability of LW/PLA composites in aqueous environments, measuring water absorption rate and thickness expansion rate. Figure 4 shows that the water absorption rate gradually increased over time, but the slope of the curve decreased, indicating a diminishing absorption rate. The rapid initial water uptake is attributed to the hemicellulose content in LW, which readily forms hydrogen bonds with water.

Figure 4a demonstrates the barrier functionality of BC, suppressing water uptake in LW/PLA composites relative to BC-free composite, while the overall absorption trend remained similar. Consistent with this, Ho et al. (2015) reported that incorporating biochar into wood composites decreased water uptake, with the extent of reduction depending on biochar particle size and loading. At 1% BC content, water absorption decreased by 6.14% relative to the control. This reduction is attributed to BC particles effectively filling microscopic pores and interfacial gaps within the LW/PLA matrix. BC obstructs water-permeable pathways, particularly within hemicellulose-rich regions of the wood flour. BC introduces non-polar surfaces that counteract the inherent hydrophilicity of hemicellulose, thereby reducing capillary action and hydrogen bonding with water molecules.

Figure 4b reveals an inverse correlation between BC loading and through-thickness swelling, achieving minimal expansion at 4 wt% BC. This demonstrates BC's efficacy in enhancing dimensional fidelity of LW/PLA composites, attributed to synergistic mechanisms: (1) intrinsic hydrophobicity acting as moisture barrier, (2) optimized polymer-filler interfacial adhesion suppressing hygroscopic stress, and (3) restricted molecular mobility reducing water plasticization.

Figure 4b reveals an inverse correlation between BC loading and through-thickness swelling, achieving minimal expansion at 4wt% BC. This demonstrates BC's efficacy in enhancing dimensional stability in composites, likely due to its inherent hydrophobicity, improved interfacial interactions with the polymer matrix, and enhanced water resistance. BC also strengthens the wood fiber-polymer matrix interfacial bond, improving stress transfer efficiency and enabling better resistance to thickness-direction swelling upon water absorption (Hoang et al., 2024).

However, Figure 4 and Table 3 reveal that BC addition had a less pronounced effect on reducing water absorption than on thickness expansion. This discrepancy may stem from BC agglomeration at higher contents, leading to non-uniform distribution within the composite. Agglomeration increases internal porosity, facilitating water molecule penetration. Structurally, poplar fibers-characterized by abundant vessels, large cell cavities, and thin cell walls—allow free water to readily enter and bind to hydroxyl groups on cell walls (Bachchan et al., 2022).

Table 3 Water absorption and thickness expansion rate at saturation.

Figure 4 Water absorption properties of BC-reinforced composites (a) Water absorption (b) Thickness expansion rate.

Three primary pathways govern moisture uptake in composites (Osa-uwagboe et al., 2024): i) Infiltration through defects (voids, micro-cracks) in the composite or matrix; ii) Matrix diffusion (following Fick's diffusion laws); iii) Capillary action along the fiber/matrix interface. To further investigate water absorption and diffusion behavior, the diffusion coefficient (*D*) of the LW/PLA composite was determined. During the initial hygroscopic stage, water absorption rate correlates positively with aging temperature under combined temperature and humidity effects. When segmental relaxation rates are slower than diffusion rates, Fick's second law applies. At this stage, moisture uptake can be expressed by Equation (4):

$$M_t = M_m(1 + k\sqrt{t})\{1 - \exp\left[-7.3\left(\frac{D_t}{h^2}\right)^{0.75}\right]\} \quad (4)$$

Where M_t represents the water absorption rate (%) at time t; M_m is the equilibrium moisture content (%); h is the thickness of the composite material (mm); k is the slope of the slant segment; *D* is the diffusion coefficient (mm^2/s).

Equation (4) can be transformed to calculate *D* (Equation 5):

$$D = \pi\left(\frac{h}{4M_m}\right)^2\left[(M_2 - M_1)/(\sqrt{t_2} - \sqrt{t_1})\right]^2 \quad (5)$$

Here, M_1 and M_2 are the moisture content of the material at any time (t_1 and t_2) of the linear section for the hygrometric curve, respectively, so they are the slope of the initial section of the M_t~ $T^{1/2}$ /h curve.

Governed by Fick's second law and considering predominant diffusion through the thickness direction (Chang et al. 2018), water absorption (M_t) was plotted against $t^{1/2}$/h (Figure 5). The initial linear region confirmed Fickian diffusion behavior, followed by an equilibrium plateau.

Figure. 5 LW/PLA composite water absorption (M_t) vs $t^{1/2}$/h curve.

As listed in Table 4, the BC-free composite exhibited the highest moisture diffusion coefficient. Increasing BC content progressively reduced diffusivity, aligning with the water absorption results. At constant temperature and diffusion medium, the diffusion coefficient relates to material density. BC addition effectively bridges interfacial gaps within the LW/PLA composite, increasing density and thereby reducing *D*. Generally, a lower diffusion coefficient indicates stronger resin-fiber interfacial adhesion and greater resistance to water diffusion, demonstrating BC's role in improving interfacial bonding. The non-monotonic variation in diffusion coefficient (D) with BC content-particularly the increase at 2% BC-may be due to localized agglomeration at intermediate loadings, which creates micro-voids and facilitates water penetration. At higher BC contents (3-4%), The positive "physical clogging and path tortuosity" effect once again surpasses the negative "defect-creation" effect, leading to a reduction in D.

Table 4 Diffusion coefficient (*D*)of BC-reinforced composites

3.2.2 BC contents on apparent color difference in composites

Color stability is a key indicator for evaluating composite aging resistance (Fabiyi et al., 2008; Liu et al., 2017). Figure 6 displays the apparent color changes of LW/PLA composites after 240-hour water immersion aging at room temperature. The BC-free composite exhibited the highest color difference *(*ΔE^* = 11.55), while ΔE^* decreased progressively with increasing BC content, reaching a minimum (ΔE^*=2.61) at 4% BC. ANOVA revealed a statistically significant difference in color change for the BC-free composite due to water absorption ($P < 0.05$), but no significant differences were observed among BC-containing composites ($P > 0.05$). Visually, composites darkened after water absorption, though BC addition mitigated this color shift.

Figure. 6 Color difference (ΔE^*) of LW/PLA composites in dry versus water-saturated states.

Table 5 Color difference parameters of LW/PLA composites after 240h water immersion.

As shown in Table 5, Δa^* and Δb^* absolute changes were minimal (<5), indicating these parameters were not primary contributors to ΔE. Higher ΔE values correspond to more severe fading and poorer aging resistance.

Figure 7a illustrates the brightness change (ΔL^*) after water aging. Higher |ΔL| indicates greater fading severity. All samples faded progressively with aging time, with the BC-free and 0.5% BC composites showing the most pronounced ΔL^* changes. Increased BC content significantly reduced ΔL^* variation. Figure 7b shows the corresponding total color difference (ΔE^*).

Figure 7 Color parameters of LW/PLA composites after water aging :(a)ΔL^*; (b)ΔE^*.

Comparison of Figures 7a and 7b reveals nearly identical trends and magnitudes between ΔL^* and ΔE^*, confirming that brightness change dominates the overall color difference. Water aging lightened composites, but appropriate BC addition effectively stabilized color. Higher BC content yielded greater color stability, attributed to: i) High-temperature processing degrades thermosensitive components in BC, leaving a chemically stable residue resistant to aging-induced changes (Igalavithana et al., 2017; X. Wang et al., 2019); ii) BC interacts effectively with composite components (consistent with Das et al.), improving overall stability and reducing water-triggered discoloration.

3.3 SEM analyze

The enhancement in hygrothermal aging resistance with BC addition indicates effective filler dispersion, which is directly visualized in the SEM micrographs (Fig. 8). Furthermore, the Fickian water absorption behavior and the concomitant mechanical degradation upon saturation are attributed to the evolution of interfacial micro-voids and cracks, as revealed by the morphological changes post-aging.

Figure 8 presents fracture morphologies in LW/PLA composites with varying BC contents (0%, 1%, 4%). In the BC-free composite (Fig. 8a), numerous voids are evident, correlating with reduced mechanical strength (20.33 MPa, Fig.2a) as these voids represent stress concentration

points. At 1% BC content (Fig. 8b), well-dispersed BC particles within the PLA matrix indicate strong interfacial compatibility. This effective reinforcement mechanism explains the peak flexural strength (25.16 MPa, Fig.2a) observed for this composition. However, at 4% BC (Fig. 8c), significant BC agglomeration creates weak interfaces. These agglomerates act as defects, leading to premature failure and the subsequent decrease in flexural strength (Fig.2a) compared to the 1% BC composite.

Figures 8d-f show fracture surfaces after water saturation. All samples exhibit rougher morphologies with discernible fiber-matrix debonding gaps, indicating water-induced debonding. This weakened interfacial bonding reduces stress transfer efficiency, explaining the observed mechanical strength reduction after water immersion (Fig.2a). Notably, the 1% BC composite maintained superior interfacial integrity compared to other formulations ((Figs. 8d & f). These observations aligns with its better retention of mechanical properties after water exposure (retained 42% strength vs. 38% for 0% and 35% for 4%), and is consistent with previous reports on water-induced interfacial damage in WPCs (Butylina et al., 2010; Beg et al., 2008).

These SEM results conclusively demonstrate that optimal interfacial compatibility and dispersion achieved at ~1% BC content, underpin the maximum dry flexural strength and the best resistance to water-induced property degradation. Higher concentrations promote agglomeration, while lower levels lack sufficient reinforcement. Therefore, maximizing PLA-fiber interfacial bonding through optimal BC addition is critical to synergistically enhance the mechanical performance and the hydrolytic stability of these composites.

Figure 8 Fracture surfaces micrographs of composites: (a-c) Dry state; (d-f) Post-water saturation. BC content: (a,d) 0%; (b,e) 1%; (c,f) 4%.

4. Conclusion

This study systematically investigated the synergistic optimization mechanism of BC addition (0.5-4 wt%) on the hygrothermal aging resistance of LW-PLA composite. The key findings are:

1. A 1wt% BC loading maximized interfacial bonding through physical anchoring and polar interactions, elevating flexural strength by 19.20% and impact resistance by 3.06% versus BC-free systems. Concurrently, dynamic mechanical analysis confirmed enhanced interfacial compatibility: 65.04% higher dry-state storage modulus and 66.67% reduced tan δ peak intensity.

2. BC-induced pore-filling and tortuous diffusion pathways reduced water absorption (↓23.35%), thickness swelling, and Fickian diffusion coefficients, mitigating moisture plasticization effects (ΔT_g = 1.2°C). Despite this, excessive BC (>1%) induced interfacial stress concentrations, degrading performance. Post-aging, flexural properties exhibited greater moisture sensitivity than impact properties (reductions of 60.25% vs. 39.57%), highlighting the preferential disruption of fiber-matrix stress transfer by hygrothermal swelling.

3. The 1 wt% BC composite achieved optimal mechanical-hygroscopic balance, peak flexural strength with minimal water uptake. This establishes a viable design paradigm for aging-resistant

sustainable building materials. These BC-reinforced LW/PLA composites, suitable for outdoor applications like decking and fencing, utilize landscaping waste and biodegradable PLA to provide a durable and eco-friendly alternative to conventional WPCs. To further advance this field, future efforts will focus on BC surface functionalization and leveraging its inherent multifunctionality for next-generation architectural composites.

Author contributions

Yu Xian: Writing – original draft, review & editing, Supervision, Conceptualization, Project administration. Shenhao Li &Xia Yang: Data curation, Conceptualization. Haixin Peng: Writing – review & editing, Conceptualization. Ruyan Zhang: Writing – original draft, Methodology, Investigation, Formal analysis. Hongbo Li &Zebing Xing: Validation, Methodology. Ge Wang &Haitao Cheng: Validation, Methodology, Project administration.

Declaration of competing interest

The author confirms the absence of any competing financial interests or personal relationships that might unduly influence this research.

Acknowledgement

This work was supported by the National Key Research and Development Program of China (No.2023YFD2202102), the Fundamental Research Program of Shanxi Province (No. 202303021221090) and Research Project of the Shanxi Scholarship Council of China (No. 2021-075). The author confirms the absence of any competing financial interests or personal relationships that might unduly influence this research.The authors gratefully acknowledge to to Ms. Zhang from Shiyanjia Lab (www.shiyanjia.com) for providing invaluable assistance with the SEM and DMA analysis.

References

Bachchan, A. A., Das, P. P., Chaudhary, V. (2022). Effect of moisture absorption on the properties of natural fiber reinforced polymer composites: A review. *Materials Today: Proceedings,* 49(p8): 3403-3408. doi:10.1016/j.matpr.2021.02.812

Bao, Y. J. J. o. T. C. M. (2018). Hydrothermal aging behaviors of CMR/PLA biocomposites. *J Thermoplast Compos Mater. 31*, 1341 - 1351. doi:10.1177/0892705717738290

Bazli, M., Heitzmann, M., Hernandez, BV. (2022). Durability of fibre-reinforced polymer-wood composite members: an overview. Compos Struct. 295:115827. https://doi. org/10.1016/j.compstruct.2022.115827.

Beg, M. D. H., Pickering, K. L.. (2008). Accelerated weathering of unbleached and bleached kraft wood fibre reinforced polypropylene composites. Polymer Degradation & Stability,#i{93}(10), 1939-1946. doi:10.1016/j.polymdegradstab.2008.06.012.

Butylina, S., Martikka, O., Karki, T. (2010). Comparison of water absorption and mechanical properties of wood–plastic composites made from polypropylene and polylactic acid. Wood Material Science & Engineering, 5(3-4), 220-228. doi:10.1080/17480272.2010.532233

Célino, A., Fréour, S., Jacquemin, F., Casari, P. (2013). The hygroscopic behavior of plant fibers: a review. Frontiers in Chemistry, 1.doi:10.3389/fchem.2013.00043.

Chang, J., Toga, K. B., Paulsen, J. D., Menon, N., Russell, T. P. (2018). Thickness dependence of the Young's modulus of polymer thin films. Macromolecules, 51(17), 6764-6770. doi:10.1021/acs.macromol.8b00602

Dahal, R. K., Acharya, B., Dutta, A. (2023). The Interaction Effect of the Design Parameters on the Water Absorption of the Hemp-Reinforced Biocarbon-Filled Bio-Epoxy Composites. *Int. J. Mol. Sci. 24*(7), 6093. doi: 10.3390/ijms24076093

Das, C., Tamrakar, S., Kiziltas, A., Xie, X. (2021). Incorporation of Biochar to Improve Mechanical, Thermal and Electrical Properties of Polymer Composites. *Polymers, 13*(16), 2663. doi:doi: 10.3390/polym13162663.

Das, O., Sarmah, A. K., Bhattacharyya, D. (2015). A novel approach in organic waste utilization through biochar addition in wood/polypropylene composites. *Waste Management, 38*, 132-140. doi:https://doi.org/10.1016/j.wasman.2015.01.015

Das, O., Sarmah, A. K., Bhattacharyya, D. (2016). Biocomposites from waste derived biochars: Mechanical, thermal, chemical, and morphological properties. *Waste Management, 49*, 560-570. doi:https://doi.org/10.1016/j.wasman.2015.12.007

Dhakal, H. N., Zhang, Z., Richardson, M. O. W. J. C. S., Technology. (2007). Effect of water absorption on the mechanical properties of hemp fibre reinforced unsaturated polyester composites. *Composites Science and Technology.* 67(7): 1674-1683. doi:https://doi.org/10.1016/j.compscitech.2006.06.019

Duigou, A. L., Davies, P., Baley, C. (2009). Seawater ageing of flax/poly(lactic acid) biocomposites. *Polymer Degradation and Stability,* 94(7), 1151-1162. doi:10.1016/j.polymdegradstab.2009.03.025.

Espinach, FX., Vilaseca, F., Tarr´es, Q. (2024). Delgado-Aguilar M, Aguado RJ, Mutj´e P. An alternative method to evaluate the micromechanics tensile strength properties of natural fiber strand reinforced polyolefin composites. The case of hemp strandreinforced polypropylene. *Compos Part B-Eng*. 273:111211. https://doi.org/ 10.1016/j.compositesb.2024.111211.

Fabiyi, J. S., McDonald, A. G., Wolcott, M. P., Griffiths, P. R. (2008). Wood plastic composites weathering: Visual appearance and chemical changes. *Polymer Degradation and Stability, 93*(8), 1405-1414. doi:https://doi.org/10.1016/j.polymdegradstab.2008.05.024

Jubinville, D., Lee, HS. Mekonnen, T. (2024) High-biocontent polymer blends and their wood plastic composites: blending, compatibilization, and their recyclability. *Appl Compos Mater* 31, 1625–1644. https://doi.org/10.1007/s10443-024-10253-w

Hao, X., Zhou, H., Mu, B., Chen, L., Ou, R. J. C. P. B. E. (2020). Effects of fiber geometry and orientation distribution on the anisotropy of mechanical properties, creep behavior, and thermal expansion of natural fiber/HDPE composites. *Composites Part B Engineering, 185*(7), 107778. doi:https://doi.org/10.1016/j.compositesb.2020.107778

Ho, M.-P., Lau, K.-T. (2014). Enhancement of impact resistance of biodegradable polymer using bamboo charcoal particles. *Materials Letters, 136*, 122-125. doi:https://doi.org/10.1016/j.matlet.2014.07.165

Ho, M.-p., Lau, K.-t., Wang, H., Hui, D. (2015). Improvement on the properties of polylactic acid (PLA) using bamboo charcoal particles. *Composites Part B: Engineering, 81*, 14-25. doi:https://doi.org/10.1016/j.compositesb.2015.05.048

Hoang, P., Zhang, Z., Ren, J., Peng, Y., Cao, J. (2024). Versatile biochar for wood-plastic composites: Improving mechanical properties, dimensional and thermal stability. *Polymer Composites,* 45(11),1-16. doi:https://doi.org/10.1002/pc.28477

Igalavithana, A. D., Mandal, S., Niazi, N. K., Vithanage, M., Parikh, S. J., Mukome, F. N. D., . . . Ok, Y. S. (2017). Advances and future directions of biochar characterization methods and applications. *Critical Reviews in Environmental Science and Technology, 47*(23), 2275-2330. doi:10.1080/10643389.2017.1421844

Jagadeesh, P., Puttegowda, M., Mavinkere Rangappa, S., Siengchin, S. J. J. o. B. E. (2023). Accelerated weathering of sustainable and micro-filler Basalt reinforced polymer biocomposites: Physical, mechanical, thermal, wettability, and water absorption studies.Journal of Building Engineering. 80,108040. doi:https://doi.org/10.1016/j.jobe.2023.108040

José S. Machado, Sara Santos, Fernando F.S. Pinho, Fábio Luís, Ana Alves, Rita Simões, José Carlos Rodrigues, (2016). Impact of high moisture conditions on the serviceability performance of wood plastic composite decks, Materials & Design.103, 122-131. https://doi.org/10.1016/j.matdes.2016.04.030.

Kamarudin, S. H., Mohd Basri, M. S., Rayung, M., Abu, F., Ahmad, S. b., Norizan, M. N., . . . Abdullah, L. C. (2022). A Review on Natural Fiber Reinforced Polymer Composites (NFRPC) for Sustainable Industrial Applications. Polymers. *14*(17), 3698. doi:10.3390/polym14173698

Li, Q., Chen, F., Sang, T. (2022). Effects of wood fiber impulse-cyclone drying process on the UV-accelerated aging properties of wood-plastic composites. *PLOS ONE, 17*(10), e0266784. doi:10.1371/journal.pone.0266784

Li, S., Wang, H., Chen, C., Li, X., Deng, Q., Li, D. (2018). Mechanical, electrical, and thermal properties of highly filled bamboo charcoal/ultra-high molecular weight polyethylene composites. *Polymer Composites, 39*(S3), E1858-E1866. doi:https://doi.org/10.1002/pc.24839

Li, X., Lei, B., Lin, Z., Huang, L., Tan, S., Cai, X. (2014). The utilization of bamboo charcoal enhances wood plastic composites with excellent mechanical and thermal properties. *Materials & Design, 53*, 419-424. doi:https://doi.org/10.1016/j.matdes.2013.07.028

Liu, X. Y., Timar, M. C., Varodi, A. M., Sawyer, G. (2017). An investigation of accelerated temperature-induced ageing of four wood species: colour and FTIR. *Wood Science and Technology, 51*(2), 357-378. doi:10.1007/s00226-016-0867-4

Lv, S., Gu, J., Tan, H., Zhang, Y. J. J. o. C. P. (2018). Enhanced durability of sustainable poly (lactic acid)-based composites with renewable starch and wood flour. Journal of Cleaner Production, 203,328-339. doi:10.1016/j.jclepro.2018.08.266

Mohammed, M., Rahman, R., Mohammed, A. M., Betar, B. O., Osman, A. F., Adam, T., Gopinath, S. C. B. (2022). Improving hydrophobicity and compatibility between kenaf fiber and polymer composite by surface treatment with inorganic nanoparticles. *Arabian Journal of Chemistry, 15*(11), 104233. doi:https://doi.org/10.1016/j.arabjc.2022.104233

Naeem, S., Baheti, V., Militky, J., Ali, A. (2017). Multifunctional polylactic acid composites filled with activated carbon particles obtained from acrylic fibrous wastes. *Polymer Composites,* 40(2),578-592. doi:10.1002/pc.24695

Oliveira, M. S., da Luz, F. S., Pereira, A. C., Costa, U. O., Bezerra, W. B. A., da Cunha, J. d. S. C., . . . Monteiro, S. N. (2022). Water Immersion Aging of Epoxy Resin and Fique Fabric Composites: Dynamic–Mechanical and Morphological Analysis.Polymers,14(17): 3650. doi: 10.3390/polym14173650

Osa-uwagboe, N., Silberschmidt, V.V. Demirci, E. (2024). Review on Mechanical Performance of Fibre-Reinforced Plastics in Marine Environments. Appl Compos Mater 31, 1991-2018 https://doi.org/10.1007/s10443-024-10247-8

Qingfa, Z., Hang, X., Xiajin, R., Wenyu, L., Haolu,L., Liang, Z., Weiming, Y. (2021). Preparation and properties of agroforestry wastes biochar/high density polyethylene composites.Acta Materiae Compositae Sinica,38(2), 398-405.doi:10.13801/j.cnki.fhclxb.20200610.004

Randhawa, K. s., Patel, A. D. J. I. L., Tribology. (2021). The effect of environmental humidity/water absorption on tribo-mechanical performance of polymers and polymer composites – a review. Industrial Lubrication and Tribology,73(9),1146-1158. doi:https://doi.org/10.1108/ILT-02-2021-0045

Saavedra-Rojas, F. A., Bhandari, S., Lopez-Anido, R. A. (2024). Environmental Durability of Bio-Based and Synthetic Thermoplastic Composites in Large-Format Additive Manufacturing.Polymers,16(6): 787.doi:10.3390/polym16060787

Shah, A. U., Imdad, A., Sadiq, A., Malik, R. A., Alrobei, H., Badruddin, I. A. (2023). Mechanical, Thermal, and Fire Retardant Properties of Rice Husk Biochar Reinforced Recycled High-Density Polyethylene Composite Material. *Polymers, 15*(8). doi:10.3390/polym15081827

Shih, H.-C., Lai, Y.-T., Yang, H.-Y., Ma, H.-w. (2024). Development of secondary material competition modelling for evaluation of incentive policies on plastic waste. *Journal of Cleaner Production, 434*, 140195. doi:https://doi.org/10.1016/j.jclepro.2023.140195

Shirinbayan, M., Nouira, S., Imaddahen, MA., Fitoussi, J. (2024). Microstructure-sensitive investigation on the plastic deformation and damage initiation of fiber-reinforced polypropylene composite. *Compos Part B-Eng*, 286:111790. https://doi.org/ 10.1016/j.compositesb.2024.111790.

Siakeng, R., Jawaid, M., Ariffin, H., Sapuan, S. M., Asim, M., Saba, N. (2019). Natural fiber reinforced polylactic acid composites: A review. *Polymer Composites, 40*(2), 446-463. doi:https://doi.org/10.1002/pc.24747

Sivamurugan, P., Mareeswaran, M., Abraar, S. A. M., Verma, S., Verma, N., Srivastava, B. K., . . . Ramesh, B. (2024). Development of thermally reduced corn stover biochar and its satin weaved sisal-reinforced vinyl ester composites. *Biomass Conversion and Biorefinery, 14*(18), 22329-22337. doi:10.1007/s13399-023-04273-y

Stark, N. M. , Matuana, L. M. (2004). Surface chemistry changes of weathered hdpe/wood-flour composites studied by xps and ftir spectroscopy. Polymer Degradation & Stability,86(1), 1-9. doi:10.1016/j.polymdegradstab.2003.11.002.

Wang, W., Guo, X., Zhao, D., Liu, L., Zhang, R., Yu, J. (2020). Water Absorption and Hygrothermal Aging Behavior of Wood-Polypropylene Composites.Polymers, *12*(4), 782. doi: 10.3390/polym12040782

Wang, X., Yu, Z., McDonald, A. (2019). Effect of Different Reinforcing Fillers on Properties, Interfacial Compatibility and Weatherability of Wood-plastic Composites. *Journal of Bionic Engineering, 16*, 337-353. doi:10.1007/s42235-019-0029-0

Wei, Y.-y., Zhang, Q.-f., Sheng, K.-c. (2022). Effect of biochar on mechanical properties of zein/polypropylene composites. J. Agric. Sci. Technol.,(10): 161-168.doi:https://doi.org/10.1016/j.conbuildmat.2019.117338

Yang, W., Wen Y., Song J. (2018). Properties of bamboo charcoal/graphite/epoxy resin electromagnetic interference shielding composite. Journal of Forestry Engineering, 3(1), 65-70.doi: 10.13360/j.issn.2096-1359.2018.01.011

Wu, Y., Xun, L., Huang, S., Ren, C., Sun, B., Gu, B. (2021). Crack spatial distributions and dynamic thermomechanical properties of 3D braided composites during thermal oxygen ageing. Composites Part A: Applied Science and Manufacturing, 144: 106355. doi:10.1016/j.compositesa.2021.106355

Xie, Y., Hill, C. A. S., Xiao, Z., Militz, H., Mai, C. (2010). Silane coupling agents used for natural fiber/polymer composites: A review. *Composites Part A: Applied Science and Manufacturing, 41*(7), 806-819. doi:https://doi.org/10.1016/j.compositesa.2010.03.005

Zhang, Q., Zhang, D., Xu, H., Lu, W., Ren, X., Cai, H., Mateo, W. (2020). Biochar filled high-density polyethylene composites with excellent properties: Towards maximizing the utilization of agricultural wastes. *Industrial Crops and Products, 146*, 112185. doi:https://doi.org/10.1016/j.indcrop.2020.112185

Zhang, Y., Cui, Y., Wang, S., Zhao, X., Wang, F., Wu, G. (2020). Effect of microwave treatment on bending properties of carbon nanotube/wood plastic composites by selective laser sintering. *Materials Letters, 267*, 127547. doi:https://doi.org/10.1016/j.matlet.2020.127547

Zhao, X., You, F. (2024). From sustainable macro debris chemical recycling to microplastic reclamation: Overview, research challenges, and outlook. *Journal of Cleaner Production, 454*, 142281. doi:https://doi.org/10.1016/j.jclepro.2024.142281

Zhou, Y., Fan, M., Chen, L. (2016). Interface and bonding mechanisms of plant fibre composites: An overview. *Composites Part B: Engineering, 101*, 31-45. doi:https://doi.org/10.1016/j.compositesb.2016.06.055

Zhu, S., Guo, Y., Chen, Y., Liu, S. (2020). Low Water Absorption, High-Strength Polyamide 6 Composites Blended with Sustainable Bamboo-Based Biochar. Nanomaterials,*10*(7), 1367. doi:https://doi.org/10.3390/nano10071367